11th International Conference on Engineering Vibration
Ljubljana, Slovenia, 7–10 September 2015

APPLICATION OF THE WAVE BASED METHOD TO STEADY-STATE VIBRATIONS OF THICK PLATES

M. Klanner*[1], K. Ellermann[2]

[1]Graz University of Technology, Institute of Mechanics, Kopernikusgasse 24/IV, 8010 Graz, Austria
michael.klanner@tugraz.at

[2]Graz University of Technology, Institute of Mechanics, Kopernikusgasse 24/IV, 8010 Graz, Austria
ellermann@tugraz.at

Keywords: Structural dynamics, Wave Based Method, Indirect Trefftz method, Mindlin plate theory, Plate bending vibrations.

Abstract. *The numerical simulation of low frequency harmonic responses of plates is usually carried out with deterministic methods, especially with the Finite Element Method (FEM), while for high frequencies statistical methods are used like the Statistical Energy Analysis (SEA). In the so-called mid-frequency region, the computational load of FEM is generally too high for practical simulations, while the assumptions of SEA are not meet. The applicability of a deterministic method called Wave Based Method (WBM) can be extended to the mid-frequency range due to a higher computational efficiency. The WBM is an indirect Trefftz method and uses exact solutions of the governing equations to approximate the unknown field variables. The method has already been developed for thin plates using the Kirchhoff plate theory, which neglects the shear deformation and rotatory inertia. A first order shear deformation theory, the Mindlin plate theory, accounts for the shear deformation and rotatory inertia and is used to extend the applicability of the WBM to thick plates. A numerical example is shown for a non-convex plate domain under point force excitation, which requires the decomposition into convex subdomains to ensure convergence. The convergence rate and computational efficiency of the WBM is compared to the FEM.*

1 INTRODUCTION

Due to government regulations and costumer requirements, the enhanced importance of noise and vibration characteristics of newly developed products needs to be taken into account in the early design phases. Therefore, efficient and accurate calculation methods are required, since virtual prototyping is commonly used in the early stages of product development.

Depending on the viewed frequency range, different kinds of methods are commonly used for the calculations. In the low frequency range, the Finite Element Method (FEM) [1] is commonly applied for the calculation of the structural vibrations, while the Boundary Element Method (BEM) [2] is used for the acoustic simulations. The efficiency of these two methods decreases with higher frequencies, since a certain number of elements per wavelength is needed to get accurate results [3].

In the high frequency range, statistical methods like the Statistical Energy Analysis (SEA) [4] become suitable for the calculation of vibration and noise. The accuracy of SEA depends on certain assumptions like high modal overlap and equipartition of energy, which are usually only fulfilled at high frequencies.

There is a gap between the low and high frequency range, for which neither the commonly used deterministic methods like FEM and BEM nor the SEA is practically suited. Many researchers developed new methods for this so-called mid-frequency gap to overcome the limitations of the classical deterministic and statistical methods. Some of these methods extend the applicability of deterministic methods to higher frequencies due to a higher calculation efficiency like the Complex Envelope Vectorization (CEV) [5] or the Variational Theory of Complex Rays (VTCR) [6]. Other methods try to reduce the assumptions of statistical methods and apply them to lower frequencies, for example the Statistical modal Energy distribution Analysis (SmEdA) [7] or the Energy Distribution Analysis (EDA) [8]. Also, hybrid methods like the Hybrid FE/SEA [9] have been developed to benefit from both types of methods.

Another deterministic method for the low and mid-frequency range is the Wave Based Method (WBM), which was developed by Desmet [10]. The WBM is an indirect Trefftz approach and has been used to calculate the harmonic response of structures and acoustic cavities. It has been applied for the interior and exterior acoustic simulation [11] and structural simulation like membrane problems and bending of thin plates [12, 13]. A complete overview of the WBM is shown in [14].

In a previous work, the authors of this paper extended the applicability of the WBM to thick plates [15]. In this paper, the results found in [15] are extended to non-convex problems and the convergence and efficiency compared to the FEM is shown. The outline of this paper is as follows: First the Mindlin theory is presented shortly, then the Wave Based Method for thick plates is described and the needed extension for non-convex problems is given. Next, a non-convex validation example is shown and the convergence and efficiency is compared to a FEM model. Finally, a conclusion is given.

2 THE MINDLIN PLATE THEORY

The Mindlin plate theory is a so-called first order shear deformation theory, which takes shear deformation and rotatory inertia into account [16]. Compared to the Kirchhoff theory, which neglects these two effects, the Mindlin plate theory is suitable for thicker plates. In [17] it is shown that the theory is quite accurate for wavelengths down to the plate thickness. The theory is described in many textbooks like [18] and a short summery is given here.

2.1 Governing Equations

In the Mindlin plate theory it is assumed that a straight line, which is normal to the middle plane in the undeformed plate, remains straight but not necessary normal to the middle surface in the deformed state. Therefore, the plate model has three degrees of freedom, the displacement of the middle surface in z-direction and the rotations about the x-axis and y-axis denoted with ψ_x and ψ_y. In Figure 1 the degrees of freedom of the plate are shown.

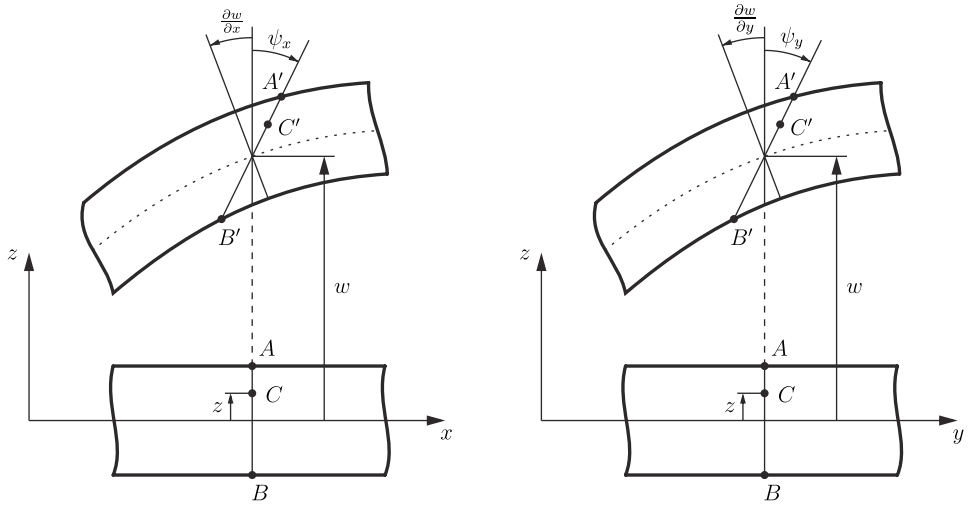

Figure 1: Degrees of freedom of the plate.

It is apparent that ψ_x is the positive rotation about the y-axis and ψ_y the negative rotation about the x-axis. Using the linear strain-displacement relations and Hook's law, the equilibrium of forces in z-direction and the equilibrium of moments about the x- and y-axis lead to the governing equations of the Mindlin plate in Cartesian coordinates

$$k^2\,G\,h\,\left(\frac{\partial^2 w}{\partial x^2}+\frac{\partial^2 w}{\partial y^2}+\Phi\right)+f=\rho\,h\,\frac{\partial^2 w}{\partial t^2}, \tag{1}$$

$$\frac{D}{2}\left[(1-\nu)\nabla^2\psi_x+(1+\nu)\frac{\partial \Phi}{\partial x}\right]-k^2\,G\,h\,\left(\psi_x+\frac{\partial w}{\partial x}\right)=\frac{\rho\,h^3}{12}\,\frac{\partial^2\psi_x}{\partial t^2}, \tag{2}$$

$$\frac{D}{2}\left[(1-\nu)\nabla^2\psi_y+(1+\nu)\frac{\partial \Phi}{\partial y}\right]-k^2\,G\,h\,\left(\psi_y+\frac{\partial w}{\partial y}\right)=\frac{\rho\,h^3}{12}\,\frac{\partial^2\psi_y}{\partial t^2}, \tag{3}$$

with $\nabla^2=\partial^2/\partial x^2+\partial^2/\partial y^2$ and $\Phi=\partial\psi_x/\partial x+\partial\psi_y/\partial y$. In Eqs. (1 - 3) G is the shear modulus, ν is the Poisson ration, h is the plate thickness, ρ is the density, $D=E\,h^3\,/\,(12\,(1-\nu^2))$ is the plate modulus, E is the elastic modulus and k^2 is the shear correction factor (Reissner $5/6$, Mindlin $\pi^2/12$) to account for the actual shear stress distribution in z-direction. An external vertical load in z-direction is denoted with f.

2.2 Decoupling of the Governing Equations

In the case of free harmonic vibrations ($f = 0$) at angular frequency ω a decoupling of the three governing equations is shown in [16]. The decoupling leads to three Helmholtz equations

$$\nabla^2 w_1 + \delta_1^2 \, w_1 = 0, \tag{4}$$

$$\nabla^2 w_2 + \delta_2^2 \, w_2 = 0, \tag{5}$$

$$\nabla^2 H + \delta_3^2 \, H = 0 \tag{6}$$

and the vertical displacement and rotations are given by

$$\psi_x = (\mu_1 - 1) \, \frac{\partial w_1}{\partial x} + (\mu_2 - 1) \, \frac{\partial w_2}{\partial x} + \frac{\partial H}{\partial y}, \tag{7}$$

$$\psi_y = (\mu_1 - 1) \, \frac{\partial w_1}{\partial y} + (\mu_2 - 1) \, \frac{\partial w_2}{\partial y} - \frac{\partial H}{\partial x}, \tag{8}$$

$$w = w_1 + w_2. \tag{9}$$

The used constants in Eqs. (4 - 9) can be found in [16].

2.3 Boundary and Interface Conditions

The Mindlin plate theory requires three boundary conditions at the plate edges to give an unique solution. The most common boundary conditions are

- kinematic boundary conditions $\boldsymbol{x} \in \tau_u$:

$$\boldsymbol{R}_u(\boldsymbol{x}) = \boldsymbol{u}(\boldsymbol{x}) - \overline{\boldsymbol{u}}(\boldsymbol{x}) = 0, \tag{10}$$

- mechanical boundary conditions $\boldsymbol{x} \in \tau_t$:

$$\boldsymbol{R}_t(\boldsymbol{x}) = \boldsymbol{t}(\boldsymbol{x}) - \overline{\boldsymbol{t}}(\boldsymbol{x}) = 0, \tag{11}$$

- mixed boundary conditions $\boldsymbol{x} \in \tau_{ut}$:

$$\boldsymbol{R}_{ut1}(\boldsymbol{x}) = \boldsymbol{u}_i(\boldsymbol{x}) - \overline{\boldsymbol{u}}_i(\boldsymbol{x}) = 0, \tag{12}$$

$$\boldsymbol{R}_{ut2}(\boldsymbol{x}) = \boldsymbol{t}_k(\boldsymbol{x}) - \overline{\boldsymbol{t}}_k(\boldsymbol{x}) = 0,$$

with $\boldsymbol{u} = [w, \psi_n, \psi_s]^T$, $\boldsymbol{t} = [Q_n, M_n, M_{ns}]^T$ and $\boldsymbol{u}_i$, $\boldsymbol{t}_k$ as the ith or kth components of $\boldsymbol{u}$ and $\boldsymbol{t}$ respectively. The plate boundary τ is divided into three non-overlapping parts τ_u, τ_t and τ_{ut} to define the three types of boundary conditions and $\boldsymbol{x}$ is the position vector at the boundaries. Q_n is the transverse shear force and M_n, M_{ns} are the bending and twisting moments, which can be defined by the displacement variables and their deviations [15]. The subscripts n and s stand for the normal and tangential direction of the plate boundary. The boundary residuals $\boldsymbol{R}_u$, $\boldsymbol{R}_t$, $\boldsymbol{R}_{ut1}$ and $\boldsymbol{R}_{ut2}$ become zero if the prescribed boundary values $\overline{\boldsymbol{u}}$ and $\overline{\boldsymbol{t}}$ are perfectly matched.

3 THE WAVE BASED METHOD

The Wave Based Method uses exact solutions of the governing equations as basic functions to describe the displacement field of the plate. Therefore, errors only occur at the boundaries of the plate and also at the interfaces in case the plate domain has to be divided into subdomains. The boundary and interface residuals are minimized in an integral sense, using a weighted residual formulation.

3.1 Field Variable Expansion

The decoupling of the governing equations in Helmholtz equations simplifies the definition of exact solutions and the variables w_1, w_2 and H are approximated with

$$w_1(x,y) \approx \tilde{w}_1(x,y) = \sum_{i_{w1}=0}^{n_{w1}} a_{i_{w1}}\, \Psi_{i_{w1}}(x,y) + \hat{w}_{1p}, \tag{13}$$

$$w_2(x,y) \approx \tilde{w}_2(x,y) = \sum_{i_{w2}=0}^{n_{w2}} a_{i_{w2}}\, \Psi_{i_{w2}}(x,y) + \hat{w}_{2p}, \tag{14}$$

$$H(x,y) \approx \tilde{H}(x,y) = \sum_{i_H=0}^{n_H} a_{i_H}\, \Psi_{i_H}(x,y) + \hat{H}_p, \tag{15}$$

with $\Psi_{i_{w1}}$, $\Psi_{i_{w2}}$ and Ψ_{i_H} as solutions of the governing equations Eqs. (4 - 6) and $\hat{w}_{1p}$, $\hat{w}_{2p}$ and $\hat{H}_p$ as particular solution functions, which satisfy the inhomogeneous part of the Eqs. (1 - 3). The used basic functions $\Psi_{i_{w1}}$, $\Psi_{i_{w2}}$ and Ψ_{i_H} are listed in Table 1 and have been derived in [15]. The dimensions of the smallest rectangular bounding box of a considered convex domain are denoted with L_x and L_y. The particular solution functions for a point force excitation are given by

$$\hat{w}_{1p} = \frac{1}{\mu_1 - 1} \frac{-\mathrm{H}_0^{(1)}(\delta_1\, r)}{D\,\sqrt{k_B^8\,(R-S)^2 + 4\,k_B^4}} \frac{j}{4}, \tag{16}$$

$$\hat{w}_{2p} = \frac{1}{\mu_2 - 1} \frac{\mathrm{H}_0^{(1)}(\delta_2\, r)}{D\,\sqrt{k_B^8\,(R-S)^2 + 4\,k_B^4}} \frac{j}{4}, \tag{17}$$

$$\hat{H}_p = 0, \tag{18}$$

with $\mathrm{H}_0^{(1)}$ the zero order Hankel function of the first kind and the distance to the excitation point r. The solutions in Eqs. (16 - 18) are the response of an infinite plate to a point force excitation [19]. The given basic functions ensure convergence for a rectangular plate domain [15], which equally ensures the convergence for a convex domain [10]. In the case of a non-convex plate domain, the domain needs to be subdivided into convex subdomains and interface conditions have to be applied.

3.2 Weighted Residual Formulation

The wave functions in Table 1 satisfy the governing equations of the Mindlin plate independently of the weighting factors $a_{i_{w1}}$, $a_{i_{w2}}$ and a_{i_H}. The weighting factors are determined by the boundary conditions and interface conditions, using a minimization of the approximation error of the boundary and interface residuals through a weighted residual formulation. The boundary residuals for a convex subdomain α of the plate are defined in Eqs. (10 - 12). The interface conditions between two connected convex plate domains α and β are defined as

$$\boldsymbol{R}_{I_u}^{(\alpha,\beta)}(\boldsymbol{x}) = \boldsymbol{u}^{(\alpha)}(\boldsymbol{x}) - \boldsymbol{u}^{(\beta)}(\boldsymbol{x}), \tag{19}$$

$$\boldsymbol{R}_{I_t}^{(\alpha,\beta)}(\boldsymbol{x}) = \boldsymbol{t}^{(\alpha)}(\boldsymbol{x}) + \boldsymbol{t}^{(\beta)}(\boldsymbol{x}). \tag{20}$$

The residuals are orthogonalized with respect to weighting functions $\hat{w}_1$, $\hat{w}_2$ and $\hat{H}$ and like in the Galerkin procedure these weighting functions are chosen as an expansion of the same basic

Table 1: Wave function sets.

	wave functions for w_1		
set 1	$\Psi_{i_{w1}} = \cos(k_{i_{w1},x}\, x)\, \exp(-j\, k_{i_{w1},y}\, y)$	$k_{i_{w1},x} = \frac{i_{w1}\,\pi}{L_x}$	$k_{i_{w1},y} = \pm\sqrt{\delta_1^2 - k_{i_{w1},x}^2}$
	$\Psi_{j_{w1}} = \exp(-j\, k_{j_{w1},x}\, x)\, \cos(k_{j_{w1},y}\, y)$	$k_{j_{w1},y} = \frac{j_{w1}\,\pi}{L_y}$	$k_{j_{w1},x} = \pm\sqrt{\delta_1^2 - k_{j_{w1},y}^2}$
set 2	$\Psi_{i_{w1}} = \sin(k_{i_{w1},x}\, x)\, \exp(-j\, k_{i_{w1},y}\, y)$	$k_{i_{w1},x} = \frac{i_{w1}\,\pi}{L_x}$	$k_{i_{w1},y} = \pm\sqrt{\delta_1^2 - k_{i_{w1},x}^2}$
	$\Psi_{j_{w1}} = \exp(-j\, k_{j_{w1},x}\, x)\, \sin(k_{j_{w1},y}\, y)$	$k_{j_{w1},y} = \frac{j_{w1}\,\pi}{L_y}$	$k_{j_{w1},x} = \pm\sqrt{\delta_1^2 - k_{j_{w1},y}^2}$
	wave functions for w_2		
set 1	$\Psi_{i_{w2}} = \cos(k_{i_{w2},x}\, x)\, \exp(-j\, k_{i_{w2},y}\, y)$	$k_{i_{w2},x} = \frac{i_{w2}\,\pi}{L_x}$	$k_{i_{w2},y} = \pm\sqrt{\delta_2^2 - k_{i_{w2},x}^2}$
	$\Psi_{j_{w2}} = \exp(-j\, k_{j_{w2},x}\, x)\, \cos(k_{j_{w2},y}\, y)$	$k_{j_{w2},y} = \frac{j_{w2}\,\pi}{L_y}$	$k_{j_{w2},x} = \pm\sqrt{\delta_2^2 - k_{j_{w1},y}^2}$
set 2	$\Psi_{i_{w2}} = \sin(k_{i_{w2},x}\, x)\, \exp(-j\, k_{i_{w2},y}\, y)$	$k_{i_{w2},x} = \frac{i_{w2}\,\pi}{L_x}$	$k_{i_{w2},y} = \pm\sqrt{\delta_2^2 - k_{i_{w2},x}^2}$
	$\Psi_{j_{w2}} = \exp(-j\, k_{j_{w2},x}\, x)\, \sin(k_{j_{w2},y}\, y)$	$k_{j_{w2},y} = \frac{j_{w2}\,\pi}{L_y}$	$k_{j_{w2},x} = \pm\sqrt{\delta_2^2 - k_{j_{w2},y}^2}$
	wave functions for H		
set 1	$\Psi_{i_H} = \sin(k_{i_H,x}\, x)\, \exp(-j\, k_{i_H,y}\, y)$	$k_{i_H,x} = \frac{i_H\,\pi}{L_x}$	$k_{i_H,y} = \pm\sqrt{\delta_3^2 - k_{i_H,x}^2}$
	$\Psi_{j_H} = \exp(-j\, k_{j_H,x}\, x)\, \sin(k_{j_H,y}\, y)$	$k_{j_H,y} = \frac{j_H\,\pi}{L_y}$	$k_{j_H,x} = \pm\sqrt{\delta_3^2 - k_{j_H,y}^2}$
set 2	$\Psi_{i_H} = \cos(k_{i_H,x}\, x)\, \exp(-j\, k_{i_H,y}\, y)$	$k_{i_H,x} = \frac{i_H\,\pi}{L_x}$	$k_{i_H,y} = \pm\sqrt{\delta_3^2 - k_{i_H,x}^2}$
	$\Psi_{j_H} = \exp(-j\, k_{j_H,x}\, x)\, \cos(k_{j_H,y}\, y)$	$k_{j_H,y} = \frac{j_H\,\pi}{L_y}$	$k_{j_H,x} = \pm\sqrt{\delta_3^2 - k_{j_H,y}^2}$

functions used for the field variable approximation. This leads to

$$\int_{\tau_u} \hat{\boldsymbol{t}}^{(\alpha)^{\boldsymbol{T}}}\, \boldsymbol{R}_u^{(\alpha)}\, \mathrm{d}\tau - \int_{\tau_t} \hat{\boldsymbol{u}}^{(\alpha)^{\boldsymbol{T}}}\, \boldsymbol{R}_t^{(\alpha)}\, \mathrm{d}\tau + \int_{\tau_{tv}} \hat{\boldsymbol{t}}^{(\alpha)^{\boldsymbol{T}}}\, \boldsymbol{R}_{tu1}^{(\alpha)}\, \mathrm{d}\tau - \tag{21}$$
$$\int_{\tau_{tv}} \hat{\boldsymbol{u}}^{(\alpha)^{\boldsymbol{T}}}\, \boldsymbol{R}_{tu2}^{(\alpha)}\, \mathrm{d}\tau + \sum_{\beta,\beta\neq\alpha} \int_{\tau_{I_u}} \hat{\boldsymbol{t}}^{(\alpha)^{\boldsymbol{T}}}\, \boldsymbol{R}_{I_u}^{(\alpha,\beta)}\, \mathrm{d}\tau - \sum_{\beta,\beta\neq\alpha} \int_{\tau_{I_t}} \hat{\boldsymbol{u}}^{(\alpha)^{\boldsymbol{T}}}\, \boldsymbol{R}_{I_t}^{(\alpha,\beta)}\, \mathrm{d}\tau = 0$$

for each convex subdomain. If Eq. (21) is evaluated for each subdomain, a system of linear equations results, which can be solved for the unknown contribution factors.

4 VALIDATION EXAMPLE

The WBM is used to calculate the displacement field of a clamped U-shaped plate and the results are compared to a reference model. The convergence rate of the WBM is compared to a FEM model built in *ANSYS*® 16.0, to show its effectiveness.

4.1 Plate configuration

The U-shaped plate is shown in Figure 2 and has a thickness h of $0.05\,m$. The plate is made of aluminium with an elasticity modulus $E = 70 \times 10^9\,N/m^2$, a Poisson ratio $\nu = 0.3$ and a density $\rho = 2790\,kg/m^3$. The shear correction factor k^2 is set to $5/6$.

A normal load $f = 1000\,N$ is acting at the point F_1 with an excitation frequency of $10000\,Hz$. The validation points P_1 - P_5, listed in Table 2, are used to compare the displacements of the WBM and the FEM. Since the plate is non-convex, it is divided into three convex subdomains Ω_1, Ω_2 and Ω_3, which is indicated by the dashed lines in Fig. 2. All edges of the plate are clamped ($\overline{\boldsymbol{u}} = 0$).

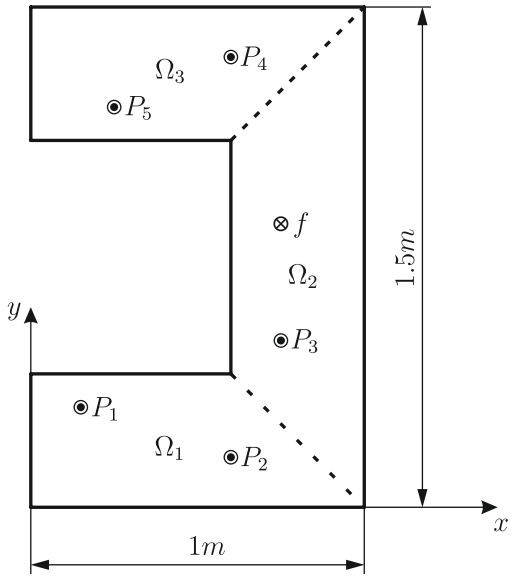

Figure 2: Geometry of the validation example.

Points	x [m]	y [m]
P_1	$0.15\,m$	$0.30\,m$
P_2	$0.60\,m$	$0.15\,m$
P_3	$0.75\,m$	$0.50\,m$
P_4	$0.60\,m$	$1.35\,m$
P_5	$0.25\,m$	$1.20\,m$
F_1	$0.75\,m$	$0.85\,m$

Table 2: Coordinates of the validation points.

The FEM reference model is meshed with the quadric 8-noded quadrilateral Shell281 element and the element size is set to $1.667\,10^{-3}\,m$. The occurring wavelength in the example is $0.165\,m$ and therefore, 100 elements per wavelength are used for the reference model. According to [20] only three quadric elements would be necessary to get accurate results.

The wave based model is built in *MATLAB*® $R2014b$. The integrals in Eqs. (21) are evaluated, using the Gauss-Legendre quadrature and the resulting system of linear equations is solved with the singular value decomposition (SVD).

4.2 Displacement results

A wave based model with 1980 wave function is used to calculate the displacements and rotations of the plate, shown in Figure 3. It is apparent that the applied boundary conditions and the interface conditions between the subdomains are well fulfilled. Therefore, the error inside the domain is small, as it will become apparent from the convergence calculations, since errors are only introduced at the boundary and interface conditions.

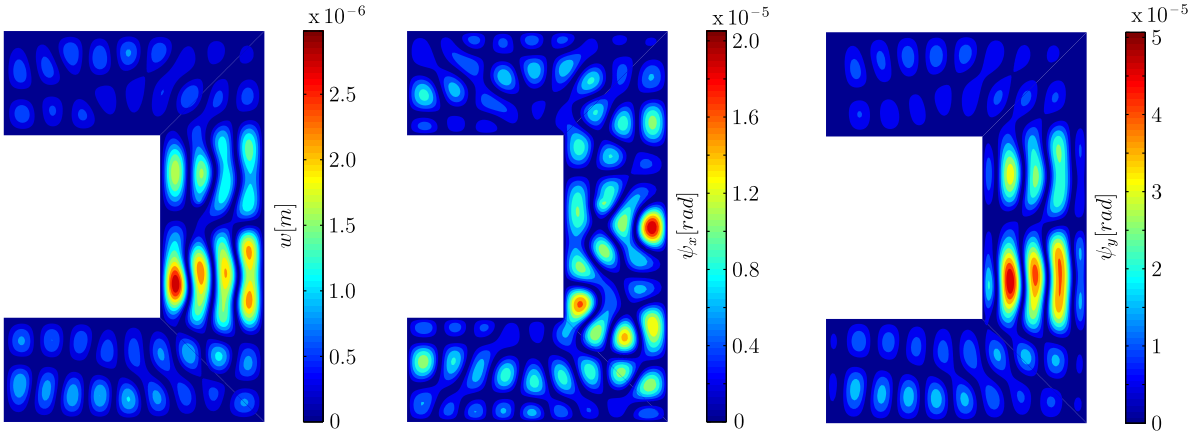

Figure 3: Displacements and rotations of the plate at 10000 Hz excitation.

The definition of the relative predicted error

$$\langle \epsilon \rangle = \frac{1}{n_P} \sum_{j=1}^{n_P} \epsilon_{Pj} \tag{22}$$

with

$$\epsilon_{Pj} = \frac{||w(\boldsymbol{x_{Pj}}) - w^{ref}(\boldsymbol{x_{Pj}})||}{||w^{ref}(\boldsymbol{x_{Pj}})||} \tag{23}$$

is used to investigate the convergence of the WBM compared to FEM. Therefore, five different numbers of wave functions (780, 900, 1380, 1740, 1980) and six different element sizes ($0.025\,m$, $0.02083\,m$, $0.0166\,m$, $0.0125\,m$, $0.01042\,m$, $0.0083\,m$) are used to calculate the displacement field. The results are shown in Figure 4.

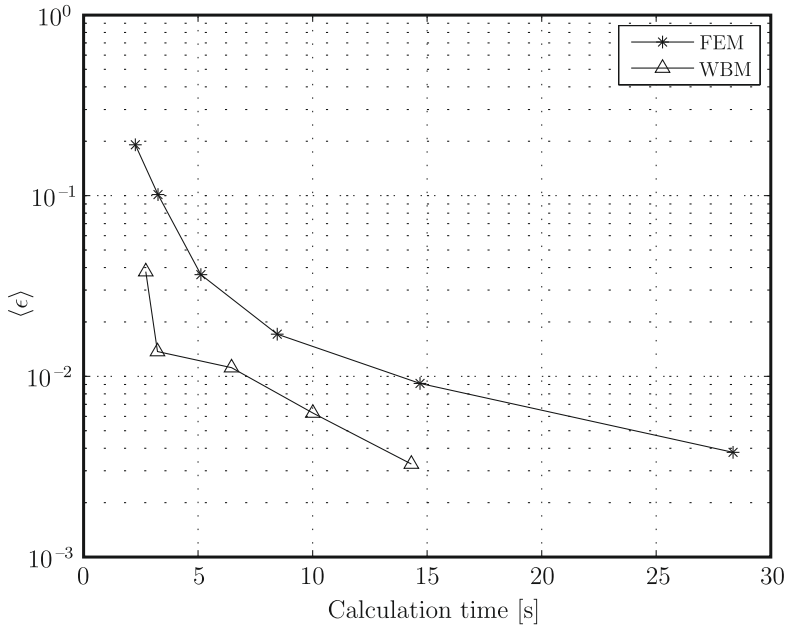

Figure 4: Convergence rate of the WBM.

The WBM has a higher computational efficiency for the given problem compared to FEM. The calculation time of the WBM could be further reduced if an optimized implementation of the WBM is used. It needs to be mentioned that for the geometry of the example plate and the chosen boundary conditions, singularities of the transverse shear force and moments occur in the two corners with obtuse angles. This has a bad influence on the convergence rate of the WBM and can be resolved by introducing special purpose functions, which account for the singularities [13]. The special purpose functions are not available for the Mindlin plate theory yet.

5 CONCLUSION

The Mindlin plate theory, which includes shear deformation and rotatory inertia, has been used to calculate the displacement field of a clamped non-convex plate. The governing equations have been solved by using the Wave Based Method, which required the decomposition of the non-convex plate into convex subdomains and the definition of interface conditions. The convergence rate of the WBM has been compared to the FEM and it has been shown that the WBM outperforms the FEM, although the WBM is implemented in *MATLAB*® $R2014b$ and is not optimized.

REFERENCES

[1] K. Bathe, *Finite Element Procedures*. Prentice-Hall, New Jersey, 2006.

[2] L. Wrobel and H. Aliabadi, *The Boundary Element Method*. Wiley, Chichester, 2002.

[3] S. Marburg, Six boundary elements per wavelength: Is that enough? *Journal of Computational Acoustics*, **10 (1)**, 25–51, 2002.

[4] R. Lyon and R. DeJong, *Theory and Application of Statistical Energy Analysis*. Butterworth-Heinemann, Newtown, 1995.

[5] O. Giannini, A. Carcaterra and A. Sestieri, High frequency vibrations analysis by the complex envelope vectorization. *The Journal of the Acoustical Society of America*, **6**, 3472–3483, 2007.

[6] P. Ladevèze, L. Arnaud, P. Rouch and C. Blanzè, The variational theory of complex rays for the calculation of medium-frequency vibrations. *Engineering Computations*, **18 (1)**, 193–214, 2001.

[7] L. Maxit and J. L. Guyader, Extension of sea model to subsystems with non-uniform modal energy distribution. *Journal of Sound and Vibration*, **265 (2)**, 337–358, 2003.

[8] G. Tanner, Dynamical energy analysis - determining wave energy distribution in vibro-acoustical structures in the high-frequency regime. *Journal of Sound and Vibration*, **320**, 1023–1038, 2009.

[9] P. J. Shorter and R. Langley, Vibro-acoustic analysis of complex systems. *Journal of Sound and Vibration*, **288 (3)**, 669–699, 2005.

[10] W. Desmet, *A wave based prediction technique for coupled vibroacoustic analysis*. Phd thesis, KU Leuven, 1998.

[11] B. Pluymers, W. Desmet, D. Vandepitte and P. Sas, Application of an efficient wave-based prediction technique for the analysis of vibro-acoustic radiation problems. *Journal of Computational and Applied Mathematics*, **168**, 353–364, 2004.

[12] C. Vanmaele, D. Vandepitte and W. Desmet, An efficient wave based prediction technique for plate bending vibrations. *Computer Methods in Applied Mechanics and Engineering*, **196**, 3178–3189, 2007.

[13] C. Vanmaele, *Development of a wave based prediction technique for the efficient analysis of low- and mid-frequency structural vibrations*. Phd thesis, KU Leuven, 2007.

[14] E. Deckers, O. Atak, L. Coox, R. D'Amico, H. Devriendt, S. Jonckheere, K. Koo, B. Pluymers, D. Vandepitte and W. Desmet, The wave based method: An overview of 15 years of research. *Wave Motion*, **51 (4)**, 550–565, 2014.

[15] M. Klanner and K. Ellermann, Wave Based Method for the Steady-State Vibrations of Thick Plates. *Journal of Sound and Vibration*, **345**, 146–161, 2015.

[16] R. D. Mindlin, Influence of rotatory inertia and shear on flexural motions of isotropic, elastic plates. *Journal of Applied Mechanics*, **18**, 31–38, 1951.

[17] L. R. F. Rose and C. H. Wang, Mindlin plate theory for damage detection: source solution. *The Journal of the Acoustical Society of America*, **116 (1)**, 154–171, 2004.

[18] S. Rao, *Vibration of Continuous Systems*. Wiley, New Jersey, 2007.

[19] L. Palermo Jr., On the fundamental solution to perform the dynamic analysis of reissner-mindlin's plates. *Boundary Element Technology*, **XV**, 2003.

[20] L. L. Thompson and P. M. Pinsky, Complex wavenumber Fourier analysis of the p-version finite element method. *Computational Mechanics*, **13 (4)**, 255–275, 1994